

## Article

# Synthesis of Novel Trisubstituted Olefin-Type Probe Molecules Containing *N*-Heterocycles and Their Application in Detection of Malononitrile

Zhao-Hua Chen <sup>1</sup>, Shi-Wei Yu <sup>1</sup>, Wen-Jin Xu <sup>1</sup>, Miao-Xin Li <sup>1</sup>, Yong Zeng <sup>1</sup>, Si-Wei Deng <sup>1</sup>, Jian-Yun Lin <sup>1,2,\*</sup> and Zhao-Yang Wang <sup>1,\*</sup> 

<sup>1</sup> School of Chemistry, South China Normal University, GDMPA Key Laboratory for Process Control and Quality Evaluation of Chiral Pharmaceuticals, Guangzhou Key Laboratory of Analytical Chemistry for Biomedicine, Key Laboratory of Theoretical Chemistry of Environment, Ministry of Education, Guangzhou 510006, China; 2021022663@m.scnu.edu.cn (Z.-H.C.); 2021022671@m.scnu.edu.cn (S.-W.Y.); xwj31916850@163.com (W.-J.X.); limiaoxin1215@163.com (M.-X.L.); 2023022676@m.scnu.edu.cn (Y.Z.); dsw766817@163.com (S.-W.D.)

<sup>2</sup> School of Mechanical and Automotive Engineering, South China University of Technology, Guangzhou 510640, China

\* Correspondence: jianyunlin@outlook.com (J.-Y.L.); wangzy@scnu.edu.cn (Z.-Y.W.); Tel.: +86-020-3931-0258 (Z.-Y.W.); Fax: +86-020-3931-0187 (Z.-Y.W.)

**Abstract:** Recently, the construction of the trisubstituted olefin-type probe molecules has elicited the attention of many researchers. However, the synthesis of the trisubstituted olefin-type probes containing two *N*-heterocycles simultaneously has been rarely reported. In this study, starting from the inexpensive mucobromic acid **1** and *N*-heterocyclic compound **2**, we first utilized a simple one-step reaction to synthesize a series of trisubstituted olefin-type compounds **3** simultaneously bearing with the structure of two *N*-heterocyclic rings in the absence of transition metal catalysts with a yield of 62–86%. The optimal reaction conditions were systematically explored, and the structure of the obtained compounds **3** were well characterized with <sup>1</sup>H NMR, <sup>13</sup>C NMR, X-ray single-crystal and HR-MS. The preliminary observation showed that, in the presence of base, mucobromic acid **1** reacts as its ring-opening structure, and the successive nucleophilic substitution reaction and Michael addition reaction can generate the target product **3**. Considering that the aldehyde group in the molecular structure of the trisubstituted olefin-type compounds **3** may react with malononitrile, we carried out some relevant investigations so as to realize the visual detection of malononitrile. Interestingly, among the products, compounds **3a–3c** can be prepared in portable test strips through a simple process and used to achieve the naked-eye detection of malononitrile in environmental systems as designed.

**Keywords:** mucobromic acid; *N*-heterocyclic compound; Michael addition reaction; trisubstituted olefin; probe; malononitrile detection; test strips



**Citation:** Chen, Z.-H.; Yu, S.-W.; Xu, W.-J.; Li, M.-X.; Zeng, Y.; Deng, S.-W.; Lin, J.-Y.; Wang, Z.-Y. Synthesis of Novel Trisubstituted Olefin-Type Probe Molecules Containing *N*-Heterocycles and Their Application in Detection of Malononitrile.

*Organics* **2024**, *5*, 46–58. <https://doi.org/10.3390/org5020004>

Received: 3 November 2023

Revised: 4 January 2024

Accepted: 28 March 2024

Published: 2 April 2024



**Copyright:** © 2024 by the authors. Licensee MDPI, Basel, Switzerland. This article is an open access article distributed under the terms and conditions of the Creative Commons Attribution (CC BY) license (<https://creativecommons.org/licenses/by/4.0/>).

## 1. Introduction

In recent years, the construction of trisubstituted olefin-type probe molecules has aroused the interest of a large number of researchers [1–3]. Usually, according to the structure of the substituent groups of double bonds of alkenes, there are roughly three kinds of trisubstituted olefin-type probe molecules [4], which can be classified into three different families such as tri(hetero)aryl substituted olefin-type molecules [5,6], trisubstituted olefin-type molecules with cyanide groups attached to the double bonds [7,8] and trisubstituted olefin-type molecules with heteroatoms attached to double bonds [9,10], respectively. Among these, the third type of probes are relatively less reported, which is challenging for their synthesis and application [11].

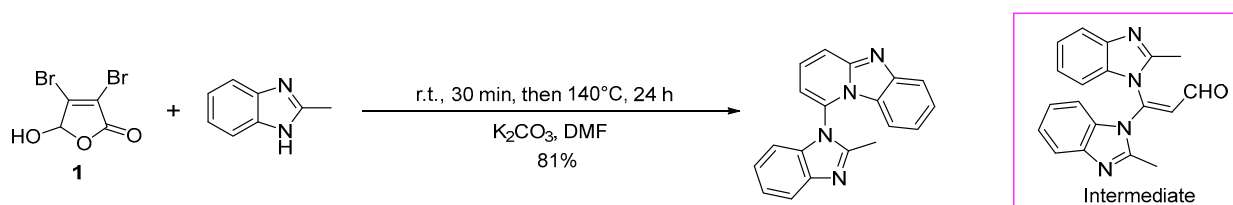
Importantly, the above-mentioned trisubstituted olefin-type probe molecules with different types of substituents, including the third type molecules [12], usually possess special properties and various applications [4,13–15]. For example, the trisubstituted olefin-type probe molecules with heteroatoms attached to olefin double bonds can be applied in many fields such as sensing picric acid (PA) [11] and detecting toxic, heavy-metal ions [16]. However, as far as we know, there are no reports on probe molecules which are constructed on the basis of the trisubstituted olefinic skeleton attaching *N*-heterocycle to olefin double bonds for the detection of malononitrile.

Malononitrile is an important chemical raw material with the merit of having excellent solubility in various organic solvents as well as water [17]. As the simplest dinitrile, malononitrile can be widely used in pharmaceutical production and industrial chemistry due to its high reactivity [18]. However, it must be noted that malononitrile is also an extremely dangerous cyanogen toxicant [19]. Malononitrile causes water pollution when it is dissolved into a water environment, where it completely converts into HCN. After entering the process of the human metabolism and animal tissues, HCN can inhibit aerobic glycolysis in tissues and the respirations of the brain, kidney and liver, causing serious diseases [20]. Eventually, this pollution caused by malononitrile can result in irreversible damage to the human body [21]. Obviously, the excessive discharge of malononitrile from chemical plants or labs, including its unreasonable and unsafe extensive use, may cause pollution to water and the surrounding environment. Unfortunately, its toxicity may also gradually accumulate in the food chain [22]. Therefore, the detection of malononitrile has begun to attract the attention of many researchers.

However, there have been limited literature reports on this subject in recent years [21,23,24]. It is well-known that the compounds within the aldehyde group can often undergo Knoevenagel condensation reactions with malononitrile [25,26]. Thus, if the colour of the compound as a probe is changed when the aldehyde group in the probe reacts with malononitrile, it can contribute to the naked-eye detection of malononitrile [24].

At the same time, our research group has also found in previous studies that most molecules based on *N*-heterocycles have excellent detection performances [27], and they have been successfully used in the detection of anions [28], cations [29] and nitroaromatic explosives (especially PA) [30], as well as pH sensing [31]. However, as far as we know, the detection of malononitrile by trisubstituted olefin-based probe molecules containing *N*-heterocycle structure has yet not been reported by any researchers.

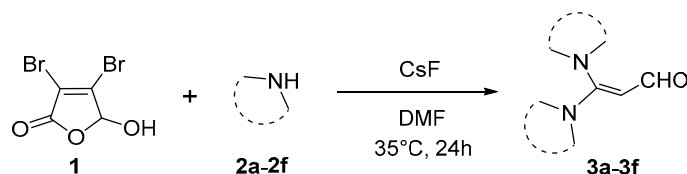
Interestingly, in our recent investigation on the synthesis of the benzazoles from mucobromic acid **1** and their application as probes for PA, when we explored the synthesis mechanism of imidazopyridines, we found that there was an intermediate compound in the form of a trisubstituted olefin molecule containing the aldehyde group during the formation of imidazopyridines (Scheme 1) [32]. Thus, we considered the fact that, if this intermediate molecule containing the aldehyde group can be easily separated and prepared by further controlling the reaction conditions, it may be of great significance to develop a simple and efficient method for the synthesis of a kind of the trisubstituted olefin-type probe molecules containing the conjugated aldehyde group.



**Scheme 1.** The synthesis route of a *N*-heterocyclic molecule probe for PA from mucobromic acid **1** and the structure of the reaction intermediate.

As expected, after the optimization of reaction conditions, we could indeed synthesize a series of compounds (**3a–3f**) starting from the cheap and easily available mucobromic acid (**1**),

and *N*-heterocycles (2) by a simple one-step reaction (Scheme 2), and their feasibility for the detection of malononitrile are also explored in this paper.



**Scheme 2.** Synthesis route of target compounds 3a–3f.

Noteworthy, due to two reasons, the chemistry of 2(5*H*)-furanone has recently attracted the attention of many researchers [33]. On the one hand, many compounds containing the structure unit of 2(5*H*)-furanone have different biological activities, giving them applications in medicine, such as anti-viral drugs [34], anti-HIV active drugs [35], inhibitors [36], and so on. Hence, research on 2(5*H*)-furanone compounds in the fields of the organic synthesis [37], natural product synthesis [38] and drug design [39] is very active. On the other hand, due to their easy availability, some simple 2(5*H*)-furanone small molecules are also important synthons in organic synthesis [40]. In fact, they can not only be used to synthesize 2(5*H*)-furanone compounds [41] but can also be utilized to prepare other functional molecules [32]. However, the latter is relatively less reported. Mucobromic acid 1 is also a simple and commercially available 2(5*H*)-furanone compound. Thus, the construction in this work of the new, functional molecules 3 based on mucobromic acid 1, namely, 3,4-dibromo-5-hydroxy-2(5*H*)-furanone can further enrich the chemistry of 2(5*H*)-furanone and has a certain application value.

## 2. Results and Discussion

### 2.1. Optimization of Reaction Conditions

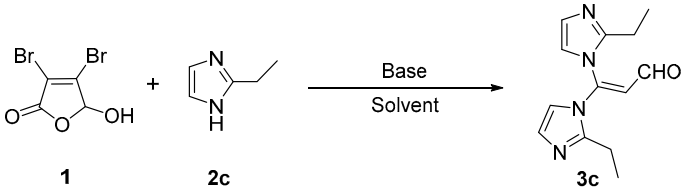
Taking the reactions of mucobromic acid (1) and ethyl imidazole (2c) as examples, we investigated the different effects of various reaction conditions (such as base type, base dosage, solvent, temperature and reaction time) on the reactions. The experimental results are summarized in Table 1.

First, we explored the effects of different inorganic bases on the reaction (Table 1, Entries 1–5). These results indicate that the product 3c can be obtained in different yields under the addition of diverse inorganic bases. Compared to inorganic bases such as sodium hydroxide, sodium carbonate, potassium carbonate and sodium bicarbonate, the best performance was achieved by using cesium fluoride (CsF) which had a yield of up to 83% (Entries 1 vs. 2–5).

Second, we investigated the effect of the equivalent of cesium fluoride on the reaction yield. According to Table 1 (Entries 1 vs. 6–7), as the amount of cesium fluoride increased from 3.0 equivalents to 4.0 equivalents, the yield was increased to 85%. However, when the amount of cesium fluoride continued to be increased to 5.0 equivalents, the yield was decreased contrarily. It can be clearly seen that an excessive increase in the amount of base is not conducive to the reaction, and using the base of 4.0 equivalents to promote the reaction results in the best yield of 85% (Entry 6).

Third, the influence of various solvents on the reaction was further studied. In comparison with other solvents, some stronger dipolar solvents, e.g., dimethyl sulfoxide (DMSO) and *N,N*-dimethylformamide (DMF), showed better reaction effects. In particular, the best reaction yield was obtained when using DMF as the solvent (Table 1, Entries 6 vs. 8–13).

According to Table 1, when the reaction temperatures are 25 °C, 35 °C, 45 °C and 55 °C, respectively, the reaction at 35 °C can give the highest yield (Entries 6 vs. 14–16). It is obvious that both raising and lowering the reaction temperature are not conducive to the progress of the reaction.

**Table 1.** Optimization of reaction conditions <sup>[a]</sup>.


| Entry    | Base (equiv.)                         | Temp. (°C) | Time (h)  | Solvent          | Yield of 3c (%) <sup>[b]</sup> |
|----------|---------------------------------------|------------|-----------|------------------|--------------------------------|
| 1        | CsF (3.0)                             | 35         | 24        | DMF              | 83                             |
| 2        | NaOH (3.0)                            | 35         | 24        | DMF              | 44                             |
| 3        | Na <sub>2</sub> CO <sub>3</sub> (3.0) | 35         | 24        | DMF              | 55                             |
| 4        | K <sub>2</sub> CO <sub>3</sub> (3.0)  | 35         | 24        | DMF              | 46                             |
| 5        | NaHCO <sub>3</sub> (3.0)              | 35         | 24        | DMF              | 47                             |
| <b>6</b> | <b>CsF (4.0)</b>                      | <b>35</b>  | <b>24</b> | <b>DMF</b>       | <b>85</b>                      |
| 7        | CsF (5.0)                             | 35         | 24        | DMF              | 78                             |
| 8        | CsF (4.0)                             | 35         | 24        | DMSO             | 70                             |
| 9        | CsF (4.0)                             | 35         | 24        | Dioxane          | <10                            |
| 10       | CsF (4.0)                             | 35         | 24        | Acetonitrile     | 30                             |
| 11       | CsF (4.0)                             | 35         | 24        | H <sub>2</sub> O | trace                          |
| 12       | CsF (4.0)                             | 35         | 24        | Toluene          | 25                             |
| 13       | CsF (4.0)                             | 35         | 24        | THF              | 28                             |
| 14       | CsF (4.0)                             | 25         | 24        | DMF              | 78                             |
| 15       | CsF (4.0)                             | 45         | 24        | DMF              | 65                             |
| 16       | CsF (4.0)                             | 55         | 24        | DMF              | 45                             |
| 17       | CsF (4.0)                             | 35         | 16        | DMF              | 48                             |
| 18       | CsF (4.0)                             | 35         | 20        | DMF              | 63                             |
| 19       | CsF (4.0)                             | 35         | 28        | DMF              | 80                             |

<sup>[a]</sup> Reaction conditions: Usually, all reactions were performed with **1** (0.20 mmol), **2c** (0.50 mmol) and solvent (2 mL), for 24 h unless there is a special statement is noted. <sup>[b]</sup> Isolated yield.

Finally, the influence of the reaction time was also investigated. It can be seen that the yield was best when the reaction time was selected as 24 h (Table 1, Entries 6 vs. 17–19).

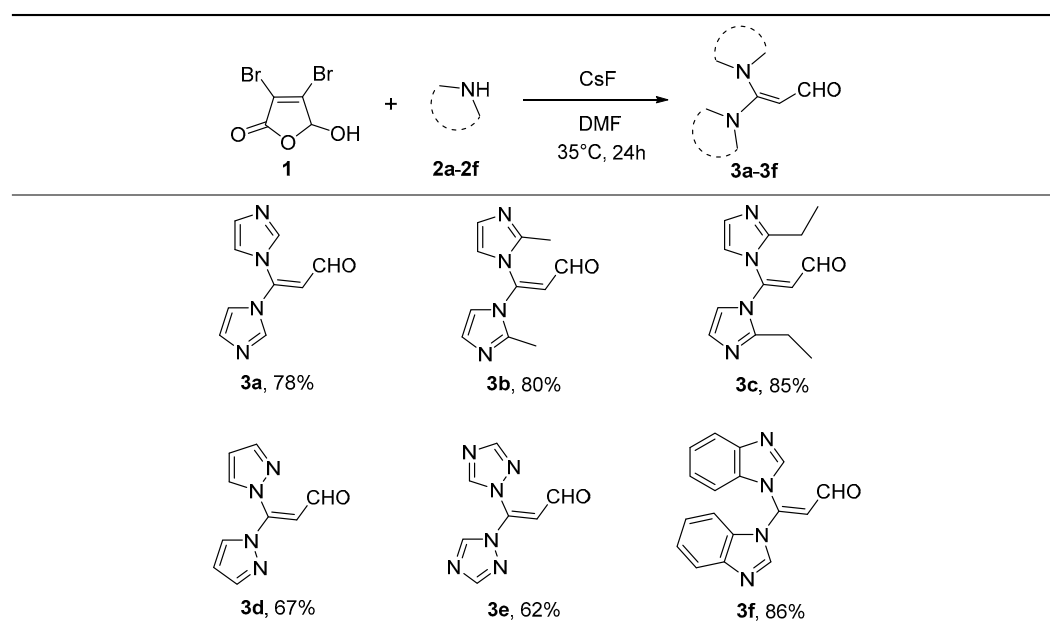
In a short, after screening, the appropriate reaction conditions for this reaction is as follows: mucobromic acid **1** (0.20 mmol), 2-ethyl imidazole **2c** (0.50 mmol) and 4.0 equivalents of cesium fluoride, with DMF as the solvent at 35 °C for 24 h, giving the separation yield of **3c** up to 85% (Table 1, Entry 6).

## 2.2. Investigation into the Range of Reaction Substrates

Using the above-optimized conditions as the reference, compounds **3a–3f** can be synthesized by utilizing different types of *N*-heterocycles **2** with mucobromic acid **1** as the starting materials. The specific substrate expansion is shown in Table 2.

These results show that, when substrates **2** are different *N*-heterocyclic compounds, such as imidazole, pyrazole, etc., the reaction can proceed smoothly, and the products **3a–3f** can be obtained in moderate to good yields (62–86%).

The general principle is that the stronger the electron donor of the *N*-heterocycles, the higher the reaction yield. In particular, the stronger the electron-donating properties of the substituents, the higher the yield. (**3c** vs. **3a**, **3b**).

**Table 2.** Substrate scope of various *N*-heterocycles **2** with mucobromic acid **1** [a,b].

[a] Reaction conditions: **1** (0.20 mmol), and **2** (0.50 mmol). CsF (0.80 mmol) and DMF (2 mL) were added and stirred at a temperature of 35 °C for 24 h. [b] Isolated yield.

Noteworthy, among the obtained compounds, **3f** with fused phenyl also has a relatively higher yield; however, due to the steric hindrance of the fused phenyl, the yield may be somewhat decreased (**3c** vs. **3f**).

If taking **3a**, **3d** and **3e** into comparison, we can easily find that the position of the nitrogen atom as well as the number of nitrogen atoms also has an influence on the reaction yield. With an increasing number of nitrogen atoms, the molecule may be more electron-withdrawing, thus contributing to a comparatively low yield.

### 2.3. Structural Characterization Analysis

From the  $^1\text{H}$  NMR of the target compound, it can be seen that the  $^1\text{H}$  NMR of the six compounds **3a-3f** are consistent with the simulated data of the hydrogen atom in the target products. For example, the  $^1\text{H}$  NMR of the synthesized compounds **3a-3f** shows that a double peak with the integration as one unit appears near 9.42 ppm, which is a characteristic peak caused by aldehyde hydrogen in the structure.

At the same time, the single peak of the chemical shift value near 189 ppm in the  $^{13}\text{C}$  NMR is also a characteristic peak of aldehyde carbon. Taken together, these test results indicate that the characterization results of  $^1\text{H}$  NMR and  $^{13}\text{C}$  NMR are consistent with expectations.

On the other hand, the molecular weights of these expected products in this experiment were obtained by high resolution mass spectrometry (HR-MS), and the error between the tested value and the calculated value was within a reasonable range. Taking compound **3c** as an example, it can be seen that the theoretical calculated value of  $[\text{M}+\text{H}]^+$  of **3c** is 245.1397, and the actual test value is 245.1394 with an error value of 0.0003, which is indeed within the reasonable range (Figure 1).

Therefore, the test characterization results of the synthesized compound **3c** are consistent with the expected values, implying that **3c** is the target compound. In conclusion, the combination of the HR-MS and NMR analyses confirms that the reactions indeed yield the expected products **3a-3f**.

Although NMR and HR-MS tests proved that compounds **3a-3f** have the expected structure, in order to further determine the structure of the product, we also conducted single-crystal cultivation of compound **3c**. Its crystal resolution data are shown in Table 3, affirming that **3c** does have the expected structure.

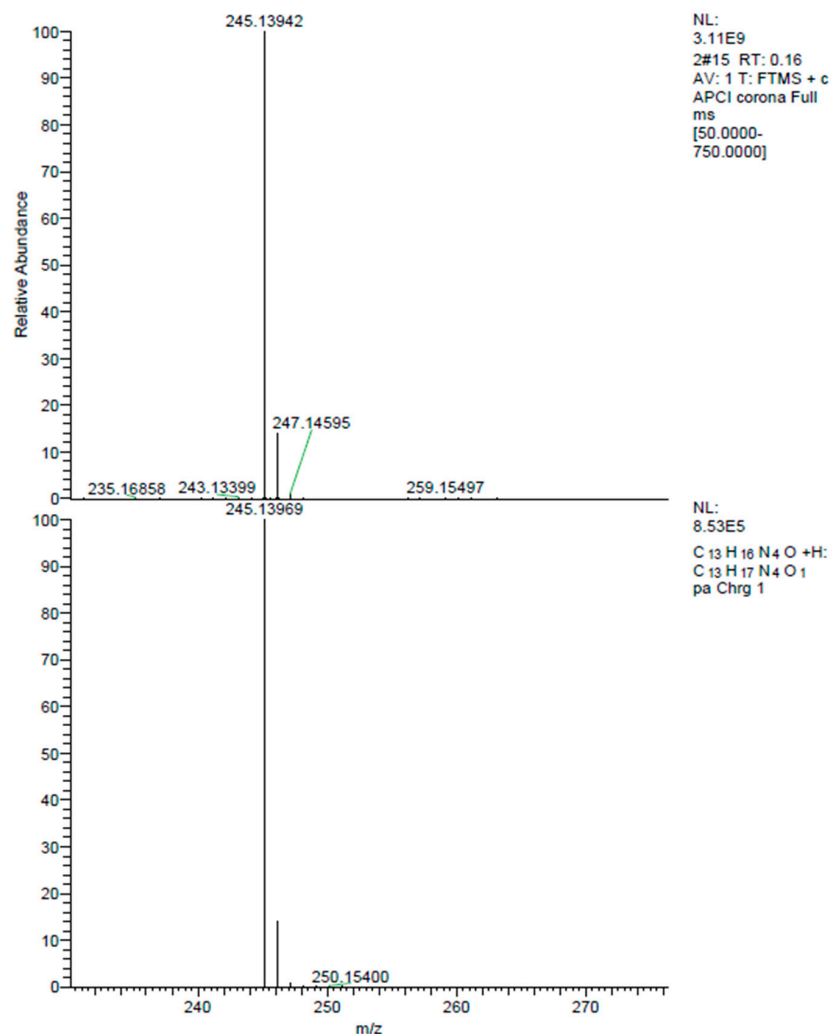


**Figure 1.** The HR-MS spectrum of compound **3c**.

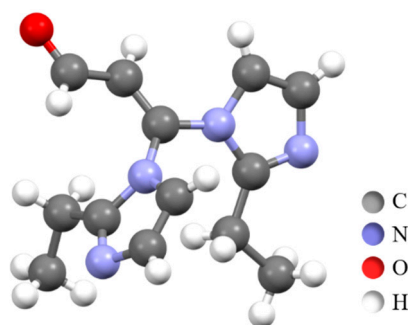
**Table 3.** X-ray crystal data and structure refinement for compound **3c**.

| Compound                        | <b>3c</b>  |
|---------------------------------|--|
| Empirical formula               | C <sub>13</sub> H <sub>16</sub> N <sub>4</sub> O   |
| Formula weight                  | 244.30   |
| Temperature (K)                 | 293 (2)  |
| Wavelength (Å)                  | 0.71073  |
| Crystal system                  | Monoclinic   |
| Space group                     | P2 <sub>1</sub> /c   |
| Unit cell dimensions (Å, °)     | $a = 9.848 (2), b = 9.0672 (16), c = 14.991 (3)$<br>$\alpha = 90, \beta = 107.02 (2), \gamma = 90$ |
| Volume (Å <sup>3</sup> )        | 1279.9 (5)   |
| Z, Density (Mg/m <sup>3</sup> ) | 4, 1.268   |
| F(000)                          | 520.0  |
| Theta range for data collection | 7.248 to 58.722°   |
| Index ranges                    | $-9 \leq h \leq 13, -12 \leq k \leq 12, -20 \leq l \leq 12$  |
| Reflections collected           | 5836   |

Table 3. Cont.

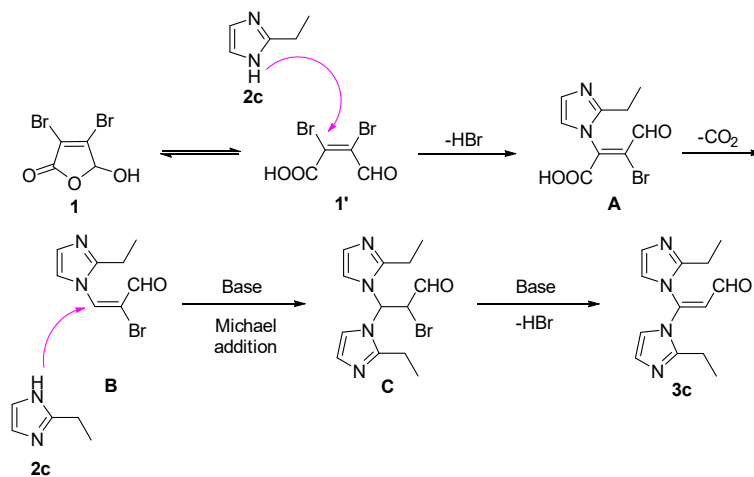
| Compound                             | 3c   |
|--------------------------------------|--|
| Independent reflections              | 2931 [ $R_{\text{(int)}} = 0.0489$ , $R_{\text{(sigma)}} = 0.0896$ ] |
| Refinement method                    | Full-matrix least-squares on $F^2$                                   |
| Data/restraints/parameters           | 2931/0/165   |
| Goodness-of-fit on $F^2$             | 1.095  |
| Final R indices [ $I > 2\sigma(I)$ ] | $R_1 = 0.0713$ , $wR_2 = 0.1296$                                     |
| R indices (all data)                 | $R_1 = 0.1486$ , $wR_2 = 0.1749$                                     |
| Largest diff. peak and hole          | 0.17 and $-0.25 \text{ e.}\text{\AA}^{-3}$                           |

Accordingly, the X-ray single-crystal diffraction results of compound **3c** in Figure 2 disclose that the molecule contains two imidazole rings and that the nitrogen atom of the two imidazole rings are connected with the same carbon atom. Moreover, the carbon atom adjacent to the previously discussed carbon atom is connected with an aldehyde group. Thus, the structure of compound **3c** can also be confirmed through the single crystal structure.

Figure 2. The crystal structure of **3c** (CCDC: 2308049).

#### 2.4. Mechanism Investigation

Based on the above experiments and substrate expansion and referring to some relevant references [42,43], in particular the reaction of mucobromic acid **1** reported by us previously [32], we believe that the plausible reaction mechanism for the formation of compounds **3a–3f** can be described in the following. Scheme 3 takes the production of compound **3c** as an example:

Scheme 3. The plausible reaction mechanism of the compound **3c**.

First, under the promotion of the base, one molecule of compound **2c** attacks the carbon atom at the  $\beta$ -position of the ring-opening structure **1'** of mucobromic acid **1**, causing a nucleophilic substitution reaction, and one molecule of hydrogen bromide is removed to form intermediate **A** [42].

Second, the intermediate **A** is decarboxylated to generate intermediate **B** [43]. Under the promotion of the inorganic base cesium fluoride, another molecule of compound **2c** attacks the intermediate **B**, and the Michael addition reaction occurs to create intermediate **C**.

Third, the further removal of one molecule of hydrogen bromide generates the target product **3c** under the action of the base.

### 2.5. Application of **3a–3c** in the Detection of Malononitrile

In accordance with the method described in the references [44,45], we prepared the solutions of compounds **3a–3f** with different concentrations ( $10^{-1}$  M~ $10^{-4}$  M) and made them into test strips. We also dissolved malononitrile in dichloromethane to prepare a solution of  $10^{-1}$  M concentration. After that, we placed one set of **3a–3f** test strips in the environment without malononitrile as the blank control, while the other set of **3a–3f** test strips was placed in the same closed space with the dichloromethane solution of malononitrile to observe the phenomena. The results are shown in Figure 3.

Interestingly, it can be found that, the test strips of compound **3c** are turned yellow after about 15 min (Figure 3c). Also significant is the fact that the lower the concentration of **3c** in the filter paper, the less obvious the yellow is. Contrarily, for the blank **3c** strips without malononitrile, there is no colour change.

The similar phenomena also can be observed for the filter papers of compounds **3a** and **3b**, but the colour changes take longer to be observed (Figure 3a,b). However, it is obvious that, even after 12 h, there are no changes for the strips of compounds **3d–3f** (Figure 3d–f).

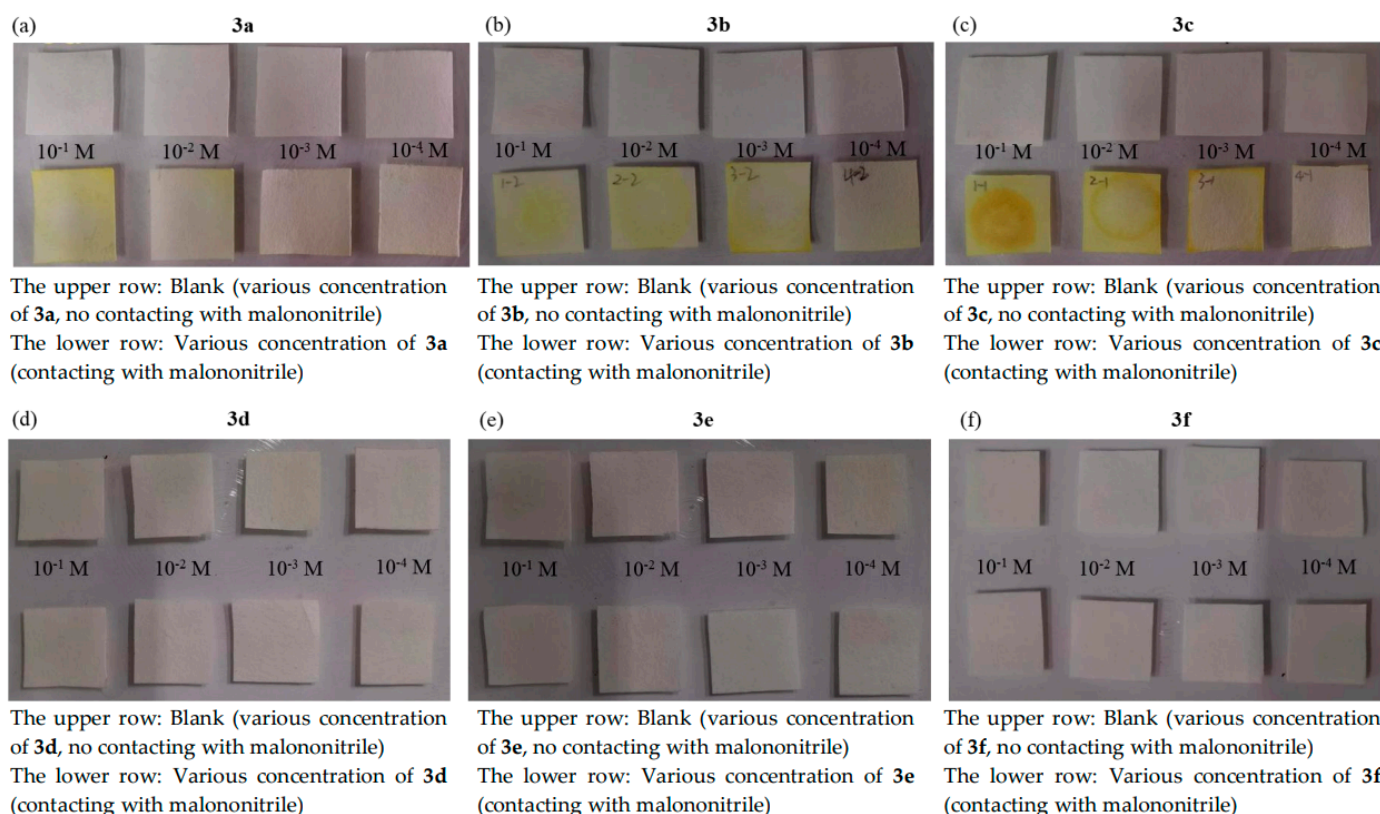


**Figure 3.** The colour changes of the test strips of compounds **3a–3f** in the environment of malononitrile ( $10^{-1}$  M).

Even when we diluted the concentration of the malononitrile environment by 100 times (making it as  $10^{-3}$  M), for compound **3a–3c**, the colour changes of the test strips can still be observed (Figure 4). However, the colour changes require a longer observation time (Table 4).

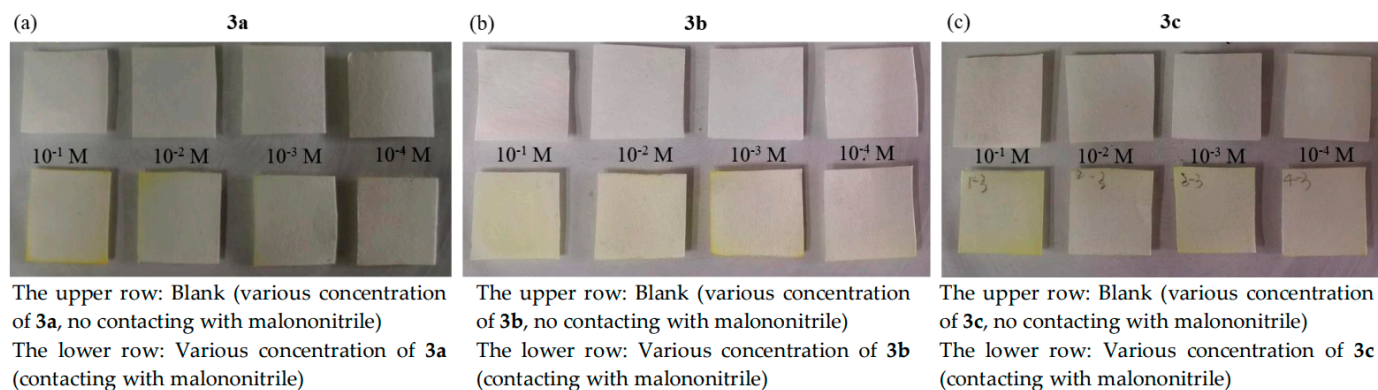


**Figure 4.** The colour changes of the test strips of compounds **3a–3c** in the environment of malononitrile ( $10^{-3}$  M).

Thus, as anticipated, it can be seen that the test strips made from the compounds **3a–3c** have certain application values for the naked-eye detection of malononitrile in the environmental system. This investigative conclusion can be expected to be applied to the qualitative detection of malononitrile when it is inevitably generated and carelessly discharged during the production processes of some chemical plants [21].

In combination with the previous results in the observation of the substrate scope, we also believe that, the position and number of nitrogen atoms in the *N*-heterocycles may affect the density distribution of the electron cloud of the heterocycle, resulting in the change of the electron effect of the heterocycle. Therefore, in some cases and especially for compounds **3d–3f**, the aldehyde group in their structure has difficulty interacting with malononitrile. At the same time, the benzimidazole ring in compound **3f** also has a larger steric hindrance than the other mono-heterocycle, which may also be unfavorable for the occurrence of the expected reaction.

**Table 4.** The minimum time for the colour changes of the test strips of compounds **3a–3f** in the malononitrile environment with different concentrations.

| Compound  | Higher Concentration ( $10^{-1}$ M)<br>Malononitrile Environment | Lower Concentration ( $10^{-3}$ M)<br>Malononitrile Environment |
|-----------|--|---|
| <b>3a</b> | 40 min   | 200 min   |
| <b>3b</b> | 30 min   | 180 min   |
| <b>3c</b> | 15 min   | 60 min  |
| <b>3d</b> | No change  | No change   |
| <b>3e</b> | No change  | No change   |
| <b>3f</b> | No change  | No change   |

### 3. Materials and Methods

#### 3.1. General Information

All compounds synthesized in this article were characterized using the AVANCE NEO-600 NMR instrument from Bruker Company (Ettlingen, Germany) by using  $\text{CDCl}_3$  as the solvent and tetramethylsilane (TMS) as the internal standard.  $^1\text{H}$  NMR was measured at 600.0 MHz, and  $^{13}\text{C}$  NMR was measured at 150.0 MHz. The high resolution mass spectrometry (HR-MS) was measured utilizing the MAT 95XP high-resolution mass spectrometry

from Thermo Fisher Scientific (Waltham, MA, USA). A single crystal of **3c** was tested by an Agilent Gemini Model E X-ray single crystal diffractometer (Santa Clara, CA, USA) (Mo as the target material).

The reaction was monitored by thin-layer chromatography (TLC) and observed under UV light at 254 nm.

All reagents and solvents in these experiments were purchased from commercial sources and directly used without further purification.

### 3.2. Experimental Procedure for the Synthesis of Compounds **3a–3f**

Firstly, 2.5 mmol of *N*-heterocycle **2** was added into a 25 mL round-bottom flask, then 3 mL dry DMF was added. In order to dissolve, the mixture was stirred at room temperature for 10 min with a magnetic stir bar. After that, 1.0 mmol of mucobromic acid **1** and 4.0 mmol of cesium fluoride were added into this flask, and the reaction was carried out for 24 h at the temperature of 35 °C.

After the reaction was completed, the obtained mixture was quenched with 15 mL H<sub>2</sub>O and was subsequently extracted with ethyl acetate (15 mL × 3). Then, the organic layers were combined and washed sequentially with saturated ammonium chloride and saturated sodium chloride aqueous solution. Next, the organic layer was dried over anhydrous Na<sub>2</sub>SO<sub>4</sub>.

After filtration and evaporation of the solvents under reduced pressure, the crude product was purified by column chromatography on silica gel to obtain the desired products **3a–3f** (Scheme 2), using ethyl acetate (EA)/petroleum ether (PE) with different ratios as eluents, respectively (for **3a**, **3b**, **3c** and **3f**, the ratio of EA/PE is 1:1; for **3d** and **3e**, the ratio of EA/PE is 1:3).

The structure of compounds **3a–3f** was well confirmed by <sup>1</sup>H NMR, <sup>13</sup>C NMR and HR-MS, while **3c** was further confirmed by single crystal characterization. The specific characterization data, including <sup>1</sup>H, <sup>13</sup>C NMR and HR-MS spectra for all compounds **3a–3f**, has been provided in Supplementary Materials.

### 3.3. Structural Characterization Data of Compounds **3a–3f**

The structures of the serial compounds **3a–3f** were systematically characterized via NMR, HR-MS, etc., and the corresponding data are summarized in the following.

(1) 3,3-Bis(1*H*-imidazol-1-yl)acrylaldehyde (**3a**), white solid (64.0 mg, 78%); m.p. 146.5–147.8 °C; <sup>1</sup>H NMR (600 MHz, CDCl<sub>3</sub>), δ, ppm: 6.17 (*d*, *J* = 7.2 Hz, 1H, CH), 7.02–7.05 (*m*, 1H, ArH), 7.19–7.24 (*m*, 2H, ArH), 7.29–7.32 (*m*, 1H, ArH), 7.64 (*s*, 1H, ArH), 7.88 (*s*, 1H, ArH), 9.43 (*d*, *J* = 7.2 Hz, 1H, CHO); <sup>13</sup>C NMR (150 MHz, CDCl<sub>3</sub>), δ, ppm: 111.8, 117.6, 120.7, 132.0, 132.5, 136.4, 139.1, 142.5, 187.8; ESI-HRMS, *m/z*: Calcd for C<sub>9</sub>H<sub>9</sub>N<sub>4</sub>O [M+H]<sup>+</sup>, 189.0771, found: 189.0769.

(2) 3,3-Bis(2-methyl-1*H*-imidazol-1-yl)acrylaldehyde (**3b**), white solid (33 mg, 80%); m.p. 166.0–168.0 °C; <sup>1</sup>H NMR (600 MHz, CDCl<sub>3</sub>), δ, ppm: 2.18 (*s*, 3H, CH<sub>3</sub>), 2.22 (*s*, 3H, CH<sub>3</sub>), 6.13 (*d*, *J* = 7.2 Hz, 1H, CH), 6.88 (*d*, *J* = 1.8 Hz, 1H, ArH), 7.07 (*d*, *J* = 1.8 Hz, 1H, ArH), 7.12 (*d*, *J* = 1.2 Hz, 1H, ArH), 7.17 (*d*, *J* = 1.2 Hz, 1H, ArH), 9.49 (*d*, *J* = 7.2 Hz, 1H, CHO); <sup>13</sup>C NMR (150 MHz, CDCl<sub>3</sub>), δ, ppm: 13.4, 14.2, 115.8, 117.2, 119.2, 122.0, 130.1, 143.5, 145.9, 146.4, 188.4; ESI-HRMS, *m/z*: Calcd for C<sub>11</sub>H<sub>13</sub>N<sub>4</sub>O [M+H]<sup>+</sup>, 217.1084, found: 217.1081.

(3) 3,3-Bis(2-ethyl-1*H*-imidazol-1-yl)acrylaldehyde (**3c**), white solid (90.3 mg, 85%); m.p. 107.0–108.0 °C; <sup>1</sup>H NMR (600 MHz, CDCl<sub>3</sub>), δ, ppm: 1.22 (*t*, *J* = 7.2 Hz, 3H, CH<sub>3</sub>), 1.26 (*t*, *J* = 7.2 Hz, 3H, CH<sub>3</sub>), 2.31–2.37 (*m*, 4H, 2CH<sub>2</sub>), 6.06 (*d*, *J* = 7.2 Hz, 1H, CH), 6.80 (*d*, *J* = 1.8 Hz, 1H, ArH), 7.04 (*d*, *J* = 1.8 Hz, 1H, ArH), 7.09 (*d*, *J* = 1.2 Hz, 1H, ArH), 7.13 (*d*, *J* = 1.2 Hz, 1H, ArH), 9.42 (*d*, *J* = 7.2 Hz, 1H, CHO); <sup>13</sup>C NMR (150 MHz, CDCl<sub>3</sub>), δ, ppm: 11.5, 11.6, 20.6, 21.1, 116.2, 119.3, 122.3, 129.8, 129.9, 143.5, 150.7, 151.1, 188.5; ESI-HRMS, *m/z*: Calcd for C<sub>13</sub>H<sub>17</sub>N<sub>4</sub>O [M+H]<sup>+</sup>, 245.1397, found: 245.1394.

(4) 3,3-Bis(1*H*-pyrazol-1-yl)acrylaldehyde (**3d**), yellow waxy (55.2 mg, 67%); <sup>1</sup>H NMR (600 MHz, CDCl<sub>3</sub>), δ, ppm: 6.49–6.52 (*m*, 2H, CH, ArH), 6.58–6.61 (*m*, 1H, ArH), 7.38 (*d*, *J* = 3.0 Hz, 1H, ArH), 7.78 (*d*, *J* = 2.4 Hz, 1H, ArH), 7.82 (*d*, *J* = 1.2 Hz, 1H, ArH), 7.89 (*d*,

$J = 1.2$  Hz, 1H, ArH), 9.53 ( $d$ ,  $J = 7.2$  Hz, 1H, CHO);  $^{13}\text{C}$  NMR (150 MHz,  $\text{CDCl}_3$ ),  $\delta$ , ppm: 109.0, 109.9, 110.8, 130.3, 133.5, 143.9, 144.7, 147.0, 189.8; ESI- HRMS,  $m/z$ : Calcd for  $\text{C}_9\text{H}_9\text{N}_4\text{O}$   $[\text{M}+\text{H}]^+$ , 189.0771, found: 189.0768.

(5) 3,3-Bis(1*H*-1,2,4-triazol-1-yl)acrylaldehyde (**3e**), yellowish waxy (51.0 mg, 62%);  $^1\text{H}$  NMR (600 MHz,  $\text{CDCl}_3$ ),  $\delta$ , ppm: 6.74 ( $d$ ,  $J = 7.2$  Hz, 1H, CH), 8.17 ( $s$ , 1H, ArH), 8.22 ( $s$ , 1H, ArH), 8.30 ( $s$ , 1H, ArH), 8.55 ( $s$ , 1H, ArH), 9.65 ( $d$ ,  $J = 6.6$  Hz, 1H, CHO);  $^{13}\text{C}$  NMR (150 MHz,  $\text{CDCl}_3$ ),  $\delta$ , ppm: 113.7, 140.1, 144.1, 146.9, 154.5, 154.6, 187.4; ESI-HRMS,  $m/z$ : Calcd for  $\text{C}_7\text{H}_7\text{N}_6\text{O}$   $[\text{M}+\text{H}]^+$ , 191.0676, found: 191.0674.

(6) 3,3-Bis(1*H*-benzo[d]imidazol-1-yl)acrylaldehyde (**3f**), yellow waxy (121.1 mg, 86%);  $^1\text{H}$  NMR (600 MHz,  $\text{CDCl}_3$ ),  $\delta$ , ppm: 6.40 ( $d$ ,  $J = 7.2$  Hz, 1H, ArH), 6.77 ( $d$ ,  $J = 7.8$  Hz, 1H, CH), 6.87 ( $d$ ,  $J = 8.4$  Hz, 1H, ArH), 7.21–7.24 ( $m$ , 2H, ArH), 7.33–7.37 ( $m$ , 2H, ArH), 7.82 ( $d$ ,  $J = 7.8$  Hz, 1H, ArH), 7.89 ( $d$ ,  $J = 7.2$  Hz, 1H, ArH), 7.94 ( $s$ , 1H, ArH), 8.20 ( $s$ , 1H, ArH), 9.55 ( $d$ ,  $J = 7.8$  Hz, 1H, CHO);  $^{13}\text{C}$  NMR (150 MHz,  $\text{CDCl}_3$ ),  $\delta$ , ppm: 110.7, 111.4, 112.5, 121.6, 121.7, 125.1, 125.2, 125.8, 125.9, 131.5, 133.2, 141.1, 141.7, 142.8, 143.8, 144.7, 188.0; ESI- HRMS,  $m/z$ : Calcd for  $\text{C}_{17}\text{H}_{13}\text{N}_4\text{O}$   $[\text{M}+\text{H}]^+$ , 289.1084, found: 289.1080.

### 3.4. Preparation of the Test Strips and the Visual Detection towards Malononitrile

Referring to the method in references [44,45], the solutions of compounds **3a–3f** with different concentrations ( $10^{-1}$ – $10^{-4}$  M) were prepared. Whatman filter paper was selected as a carrier and immersed in the above-prepared solution. Then, the filter paper was removed and dried in an air environment, while several strips of paper with a width of 1.5 cm were cut out for testing, thus giving us various test strips for probes at different concentrations.

Subsequently, we dissolved malononitrile in dichloromethane into solutions with a concentration of  $10^{-1}$  M. After that, we placed one group of test strips of compounds **3a–3f** in the environment without malononitrile as a blank control group, while keeping the other group of test strips of compounds **3a–3f** in the same closed space with the dichloromethane solution of malononitrile to observe the phenomenon.

## 4. Conclusions

In summary, we proposed a simple one-step reaction to synthesize a series of trisubstituted olefin-type compounds **3a–3f** through the promotion of the inorganic base CsF with the dipolar solvent DMF and systematically characterized their structures using NMR, HR-MS, and X-ray single-crystal. This method is effortless with mild reaction conditions and provides a new approach for the synthesis of some specific trisubstituted olefins while simultaneously bearing with the structure of two *N*-heterocyclic rings. In particular, the test strips prepared from compounds **3a–3c** can be further applied to the detection of malononitrile, thus providing a new methodology for molecular design in detecting malononitrile.

**Supplementary Materials:** The following supporting information can be downloaded at <https://www.mdpi.com/article/10.3390/org5020004/s1> and contains the  $^1\text{H}$ ,  $^{13}\text{C}$  NMR and HR-MS spectra for all compounds **3a–3f**.

**Author Contributions:** Conceptualization, Z.-Y.W.; methodology, Z.-H.C. and S.-W.Y.; formal analysis, S.-W.Y. and W.-J.X.; data curation, M.-X.L.; validation, Y.Z.; writing—original draft preparation, Z.-H.C.; writing—review and editing, S.-W.D. and Z.-Y.W.; project administration, J.-Y.L. and Z.-Y.W.; funding acquisition, Z.-Y.W. All authors have read and agreed to the published version of the manuscript.

**Funding:** This research was supported by the Guangdong Basic and Applied Basic Research Foundation (No.2021A1515012342), National Natural Science Foundation of China (20772035).

**Data Availability Statement:** All data supporting the findings of this study are available within the paper and within its Supplementary Materials published online.

**Conflicts of Interest:** The authors declare no conflicts of interest.

## References

1. Tang, Y.J.; Zhang, D.; Zhang, Y.X.; Liu, Y.L.; Cai, L.R.; Plaster, E.; Zheng, J. Fundamentals and exploration of aggregation-induced emission molecules for amyloid protein aggregation. *J. Mater. Chem. B* **2022**, *10*, 2280–2295. [[CrossRef](#)] [[PubMed](#)]
2. Zhao, Z.X.; Zhang, L.L.; Zhao, Y.; Li, Y.J.; Shi, J.B.; Zhi, J.E.; Dong, Y.P. Helical self-assembly and Fe<sup>3+</sup> detection of V-shaped AIE-active chiral tetraphenylbutadiene-based polyamides. *Chem.-Eur. J.* **2023**, *29*, e202301035. [[CrossRef](#)] [[PubMed](#)]
3. Yu, G.-H.; Hu, H.-R.; Liu, R.-B.; Sheng, G.-Z.; Niu, J.-J.; Fang, Y.; Wang, K.-P.; Hu, Z.-Q. A triphenylamine-based fluorescence probe for detection of hypochlorite in mitochondria. *Spectrochim. Acta Part A* **2023**, *299*, 122830. [[CrossRef](#)] [[PubMed](#)]
4. Chen, Z.-H.; Cao, X.-Y.; Chen, S.-H.; Yu, S.-W.; Lin, Y.-L.; Lin, S.-T.; Wang, Z.-Y. Design, synthesis and application of trisubstituted olefinic aggregation-induced emission molecules. *Chin. J. Org. Chem.* **2022**, *42*, 2355–2363. [[CrossRef](#)]
5. Jia, Y.J.; Guo, S.S.; Han, Q.Z.; Zhu, J.L.; Zhang, X.L.; Na, N.; Ouyang, J. Target-triggered and controlled release plasmon-enhanced fluorescent AIE probe for conformational monitoring of insulin fibrillation. *J. Mater. Chem. B* **2021**, *9*, 5128–5135. [[CrossRef](#)] [[PubMed](#)]
6. Duan, Y.C.; Gao, Y.; Pan, Q.Q.; Zhao, Z.W.; Wu, Y.; Zhao, L.; Geng, Y.; Su, Z.M. Whether the combination of AIE and TADF functional groups produces AIE-type TADF? A theoretical study on the synergistic effect of TPE and carbazole donor group/thianthrene-tetraoxide acceptor group. *Dyes Pigm.* **2021**, *194*, 109547. [[CrossRef](#)]
7. Chen, C.; Gao, H.Q.; Ou, H.L.; Kwok, R.T.K.; Tang, Y.H.; Zheng, D.H.; Ding, D. Amplification of activated near-infrared afterglow luminescence by introducing twisted molecular geometry for understanding neutrophil-involved diseases. *J. Am. Chem. Soc.* **2022**, *144*, 3429–3441. [[CrossRef](#)] [[PubMed](#)]
8. Kachwal, V.; Laskar, I.R. Mechanofluorochromism with aggregation-induced emission (AIE) characteristics: A perspective applying isotropic and anisotropic force. *Top. Curr. Chem.* **2021**, *379*, 28. [[CrossRef](#)] [[PubMed](#)]
9. Liu, Y.; Wolstenholme, C.H.; Carter, G.C.; Liu, H.B.; Hu, H.; Grainger, L.S.; Miao, K.; Fares, M.; Hoelzel, C.A.; Yennawar, H.P.; et al. Modulation of fluorescent protein chromophores to detect protein aggregation with turn-on fluorescence. *J. Am. Chem. Soc.* **2018**, *140*, 7381–7384. [[CrossRef](#)]
10. Biesen, L.; May, L.; Nirmalanathan-Budau, N.; Hoffmann, K.; Resch-Genger, U.; Müller, T.J.J. Communication of bichromophore emission upon aggregation-Aroyl-S,N-ketene acetals as multifunctional sensor merocyanines. *Chem. Eur. J.* **2021**, *27*, 13426. [[CrossRef](#)]
11. Wang, B.-W.; Jiang, K.; Li, J.-X.; Luo, S.-H.; Wang, Z.-Y.; Jiang, H.-F. 1,1-Diphenyl-vinylsulfide as a functional AIEgen derived from the aggregation-caused-quenching molecule 1,1-diphenylethene through simple thioetherification. *Angew. Chem. Int. Ed.* **2020**, *59*, 2338–2343. [[CrossRef](#)] [[PubMed](#)]
12. Zhang, J.W.; Wang, E.F.; Zhou, Y.; Zhang, L.; Chen, M.; Lin, X.R. A metal-free synthesis of 1,1-diphenylvinylsulfides with thiols via thioetherification under continuous-flow conditions. *Org. Chem. Front.* **2020**, *7*, 1490–1494. [[CrossRef](#)]
13. Xiao, P.H.; Ma, K.; Kang, M.M.; Huang, L.Y.; Wu, Q.; Song, N.; Ge, J.Y.; Li, D.; Dong, J.X.; Wang, L.; et al. An aggregation-induced emission platform for efficient Golgi apparatus and endoplasmic reticulum specific imaging. *Chem. Sci.* **2021**, *12*, 13949–13957. [[CrossRef](#)] [[PubMed](#)]
14. Dominguez, R.; Navarro, A.; Garcia-Martinez, J.C. Styrylbenzene organogels and how the cyano groups tune the aggregation-induced emission. *Dyes Pigm.* **2021**, *192*, 109427. [[CrossRef](#)]
15. Tian, J.W.; Teng, M.Z.; Song, M.; Li, Z.J.; Zhang, X.Y.; Xu, Y.Q. A feasible molecular engineering for bright  $\pi$ -conjugation free radical photosensitizers with aggregation-induced emission. *Dyes Pigm.* **2021**, *194*, 109651. [[CrossRef](#)]
16. Liu, B.B.; He, W.; Lu, H.; Wang, K.; Huang, M.M.; Kwok, R.T.K.; Lam, J.W.Y.; Gao, L.C.; Yang, J.P.; Tang, B.Z. A facile design for multifunctional AIEgen based on tetraaniline derivatives. *Sci. China Chem.* **2019**, *62*, 732–738. [[CrossRef](#)]
17. Jung, Y.; Park, N.K.; Kang, S.; Huh, Y.; Jung, J.; Hur, J.K.; Kim, D. Latent turn-on fluorescent probe for the detection of toxic malononitrile in water and its practical applications. *Anal. Chim. Acta* **2020**, *1095*, 154–161. [[CrossRef](#)] [[PubMed](#)]
18. Sharma, V.; Sahu, B.; Das, U.K.; Patra, G.K. A reversible fluorescent-colorimetric malononitrile based novel Schiff-base chemosensor for visual detection of bicarbonate ion in aqueous solution. *Inorg. Chim. Acta* **2023**, *552*, 121491. [[CrossRef](#)]
19. Li, M.X.; Gao, Y.; Zhang, Y.; Gong, S.; Tian, X.C.; Yang, Y.Q.; Xu, X.; Wang, Z.L.; Wang, S.F. A novel ratiometric fluorescent chemosensor for detecting malononitrile and application assisted with smartphone. *Spectrochim. Acta Part A* **2021**, *262*, 120135. [[CrossRef](#)] [[PubMed](#)]
20. Karalliedde, L.; Wheeler, H.; Maclehorse, R.; Murray, V. Possible immediate and long-term health effects following exposure to chemical warfare agents. *Public Health* **2000**, *114*, 238–248. [[CrossRef](#)] [[PubMed](#)]
21. Tu, L.P.; Liu, J.; Zhang, Z.C.; Qi, Q.R.; Yao, S.; Huang, W.C. A Michael addition reaction-based fluorescent probe for malononitrile detection and its applications in aqueous solution, living cells and zebrafish. *Analyst* **2021**, *146*, 2221–2228. [[CrossRef](#)] [[PubMed](#)]
22. Haouzi, P.; McCann, M.; Tubbs, N.; Judenherc-Haouzi, A.; Cheung, J.; Bouillaud, F. Antidotal effects of the phenothiazine chromophore methylene blue following cyanide intoxication. *Toxicol. Sci.* **2019**, *170*, 82–94. [[CrossRef](#)] [[PubMed](#)]
23. Gong, Y.; Guo, X.J.; Teng, B.H.; Zhang, Q.; Zhang, P.; Ding, C.F. Ratiometric fluorescent strategy for malononitrile determination in organic and aqueous medium and biological imaging. *Dyes Pigm.* **2021**, *184*, 108859. [[CrossRef](#)]
24. Wang, X.; Cheng, S.Y.; Liu, C.Y.; Zhang, Y.; Su, M.J.; Rong, X.D.; Zhu, H.C.; Yu, M.H.; Sheng, W.L.; Zhu, B.C. Discovery of a highly selective and ultra-sensitive colorimetric fluorescent probe for malononitrile and its applications in living cells and zebrafish. *New J. Chem.* **2022**, *46*, 1713–1719. [[CrossRef](#)]

25. Wang, W.F.; Luo, M.; Yao, W.W.; Ma, M.T.; Pullarkat, S.A.; Xu, L.; Leung, P.H. Catalyst-free and solvent-free cyanosilylation and Knoevenagel condensation of aldehydes. *ACS Sustain. Chem. Eng.* **2019**, *7*, 1718–1722. [[CrossRef](#)]
26. Das, S.; Das, P.P.; Walton, J.W.; Quah, C.K.; Ghoshal, K.; Bhattacharyya, M. Aggregation-induced emission switch showing high contrast mehanofluorochromism and solvatofluorochromism: Specifically detects  $\text{HSO}_3^-$  over bar in bioimaging studies. *Dyes Pigm.* **2023**, *217*, 111413. [[CrossRef](#)]
27. Pang, C.-M.; Cao, X.-Y.; Xiao, Y.; Luo, S.-H.; Chen, Q.; Zhou, Y.-J.; Wang, Z.-Y. N-alkylation briefly constructs tunable multifunctional sensor materials: Multianalyte detection and reversible adsorption. *iScience* **2021**, *24*, 103126. [[CrossRef](#)] [[PubMed](#)]
28. Wu, Y.-C.; Huo, J.-P.; Cao, L.; Ding, S.; Wang, L.-Y.; Cao, D.-R.; Wang, Z.-Y. Design and application of tri-benzimidazolyl star-shape molecules as fluorescent chemosensors for the fast-response detection of fluoride ion. *Sens. Actuators B* **2016**, *237*, 865–871. [[CrossRef](#)]
29. Chen, S.-H.; Jiang, K.; Liang, Y.-H.; He, J.-P.; Xu, B.-J.; Chen, Z.-H.; Wang, Z.-Y. Fine-tuning benzazole-based probe for the ultrasensitive detection of  $\text{Hg}^{2+}$  in water samples and seaweed samples. *Food Chem.* **2023**, *428*, 136800. [[CrossRef](#)] [[PubMed](#)]
30. Chen, S.-H.; Chen, Z.-H.; Jiang, K.; Cao, X.-Y.; Chen, L.-Y.; Ouyang, J.; Wang, Z.-Y. Regulating donor-acceptor system toward highly efficient dual-state emission for sensitive response of nitroaromatic explosives. *Spectrochim. Acta Part A* **2023**, *300*, 122905. [[CrossRef](#)] [[PubMed](#)]
31. Wu, Y.-C.; You, J.-Y.; Jiang, K.; Wu, H.-Q.; Xiong, J.-F.; Wang, Z.-Y. Novel benzimidazole-based ratiometric fluorescent probes for acidic pH. *Dyes Pigm.* **2018**, *149*, 1–7. [[CrossRef](#)]
32. Yang, K.; Chen, Z.-X.; Zhou, Y.-J.; Chen, Q.; Yu, S.-W.; Luo, S.-H.; Wang, Z.-Y. Simple inorganic base promoted polycyclic construction using mucohalic acid as a C-3 synthon: Synthesis and AIE probe application of benzo[4,5]imidazo[1,2-a]pyridines. *Org. Chem. Front.* **2022**, *9*, 1127–1136. [[CrossRef](#)]
33. Yu, S.L.; Hong, C.; Liu, Z.; Zhang, H. Cobalt-catalyzed vinylic C-H addition to formaldehyde: Synthesis of butenolides from acrylic acids and HCHO. *Org. Lett.* **2021**, *23*, 8359–8364. [[CrossRef](#)] [[PubMed](#)]
34. Byczek-Wyrostek, A.; Kitel, R.; Rumak, K.; Skonieczna, M.; Kasprzycka, A.; Walczak, K. Simple 2(5H)-furanone derivatives with selective cytotoxicity towards non-small cell lung cancer cell line A549—synthesis, structure-activity relationship and biological evaluation. *Eur. J. Med. Chem.* **2018**, *150*, 687–697. [[CrossRef](#)] [[PubMed](#)]
35. Bailly, F.; Queffelec, C.; Mbemba, G.; Mouscadet, J.-F.; Pommery, N.; Pommery, J.; Henichart, J.-P.; Cotelle, P. Synthesis and biological activities of a series of 4, 5-diaryl-3-hydroxy-2(5H)-furanones. *Eur. J. Med. Chem.* **2008**, *43*, 1222–1229. [[CrossRef](#)] [[PubMed](#)]
36. Pinheiro, J.; Lyons, T.; Heras, V.L.; Recio, M.V.; Gahan, C.G.M.; O’Sullivan, T.P. Investigation of halogenated furanones as inhibitors of quorum sensing-regulated bioluminescence in *Vibrio harveyi*. *Future Med. Chem.* **2023**, *15*, 317–332. [[CrossRef](#)] [[PubMed](#)]
37. Valle-Amores, M.A.; Feberero, C.; Martin-Somer, A.; Díaz-Tendero, S.; Smith, A.D.; Fraile, A.; Alemán, J. Intramolecular hydrogen bond activation for kinetic resolution of furanone derivatives by an organocatalyzed [3+2] asymmetric cycloaddition. *Org. Chem. Front.* **2024**, *11*, 1028–1038. [[CrossRef](#)]
38. Papidocha, S.M.; Bulthaupt, H.H.; Carreira, E.M. Synthesis of neocaesalpin A, AA, and nominal neocaesalpin K. *Angew. Chem. Int. Ed.* **2023**, *62*, e202310149. [[CrossRef](#)] [[PubMed](#)]
39. Irie, T.; Asami, T.; Sawa, A.; Uno, Y.; Hanada, M.; Taniyama, C.; Funakoshi, Y.; Masai, H.; Sawa, M. Discovery of novel furanone derivatives as potent Cdc7 kinase inhibitors. *Eur. J. Med. Chem.* **2017**, *130*, 406–418. [[CrossRef](#)] [[PubMed](#)]
40. Wang, Y.Z.; Yu, Y.D.; Yu, Y.; Huang, F.; Baell, J.B. Copper-catalyzed olefinic C(sp<sup>2</sup>)-H activation/carbene insertion/ester hydrolysis/cyclization with aryl diazo esters for the synthesis of multisubstituted furanones. *Adv. Synth. Catal.* **2023**, *365*, 2601–2606. [[CrossRef](#)]
41. Lepage, M.L.; Alachouzos, G.; Hermens, J.G.H.; Elders, N.; van den Berg, K.J.; Feringa, B.L. Electron-poor butenolides: The missing link between acrylates and maleic anhydride in radical polymerization. *J. Am. Chem. Soc.* **2023**, *145*, 17211–17219. [[CrossRef](#)] [[PubMed](#)]
42. Teng, Q.-H.; Peng, X.-J.; Mo, Z.-Y.; Xu, Y.-L.; Tang, H.-T.; Wang, H.-S.; Sun, H.-B.; Pan, Y.-M. Transition-metal-free C-N and C-C formation: Synthesis of benzo[4,5]imidazo[1,2-a]pyridines and 2-pyridones from ynones. *Green Chem.* **2018**, *20*, 2007–2012. [[CrossRef](#)]
43. Feng, B.-B.; Lu, L.; Li, C.; Wang, X.-S. Iodine-catalyzed synthesis of dibenzo[b,h][1,6]-naphthyridine-11-carboxamides via a domino reaction involving double elimination of hydrogen bromide. *Org. Biomol. Chem.* **2016**, *14*, 2774–2779. [[CrossRef](#)] [[PubMed](#)]
44. Kumar, G.G.V.; Bhaskar, R.; Harathi, J.; Jayaprakash, N. Selective colorimetric signaling of mercury (II) ions using a quinoline-based probe with INHIBIT logic gate behavior and test strip. *Inorg. Chem. Commun.* **2023**, *148*, 110364. [[CrossRef](#)]
45. Ozturk, D.; Omeroglu, I.; Koksoy, B.; Gol, C.; Durmus, M. A BODIPY decorated multiple mode reusable paper-based colorimetric and fluorometric pH sensor. *Dyes Pigm.* **2022**, *205*, 110510. [[CrossRef](#)]

**Disclaimer/Publisher’s Note:** The statements, opinions and data contained in all publications are solely those of the individual author(s) and contributor(s) and not of MDPI and/or the editor(s). MDPI and/or the editor(s) disclaim responsibility for any injury to people or property resulting from any ideas, methods, instructions or products referred to in the content.